



# Four Molybdenum-Dependent Steroid C-25 Hydroxylases: Heterologous Overproduction, Role in Steroid Degradation, and Application for 25-Hydroxyvitamin D<sub>3</sub> Synthesis

Christian Jacoby,<sup>a</sup> Jens Eipper,<sup>a</sup> Markus Warnke,<sup>a</sup> Oliver Tiedt,<sup>a</sup> Mario Mergelsberg,<sup>a</sup> Hans-Joachim Stärk,<sup>b</sup> Birgit Daus,<sup>b</sup> Zaira Martín-Moldes,<sup>c</sup> María Teresa Zamarro,<sup>c</sup> Eduardo Díaz,<sup>c</sup>  Matthias Boll<sup>a</sup>

<sup>a</sup>Faculty of Biology–Microbiology, Albert-Ludwigs-Universität Freiburg, Freiburg, Germany

<sup>b</sup>Department of Analytical Chemistry, Helmholtz Centre for Environmental Research UFZ, Leipzig, Germany

<sup>c</sup>Department of Microbial and Plant Biotechnology, Centro de Investigaciones Biológicas, CSIC, Madrid, Spain

**ABSTRACT** Side chain-containing steroids are ubiquitous constituents of biological membranes that are persistent to biodegradation. Aerobic, steroid-degrading bacteria employ oxygenases for isoprenoid side chain and tetracyclic sterane ring cleavage. In contrast, a Mo-containing steroid C-25 dehydrogenase (S25DH) of the dimethyl sulfoxide (DMSO) reductase family catalyzes the oxygen-independent hydroxylation of tertiary C-25 in the anaerobic, cholesterol-degrading bacterium *Sterolibacterium denitrificans*. Its genome contains eight paralogous genes encoding active site  $\alpha$ -subunits of putative S25DH-like proteins. The difficult enrichment of labile, oxygen-sensitive S25DH from the wild-type bacteria and the inability of its active heterologous production have largely hampered the study of S25DH-like gene products. Here we established a heterologous expression platform for the three structural genes of S25DH subunits together with an essential chaperone in the denitrifying betaproteobacterium *Thauera aromatica* K172. Using this system, S25DH<sub>1</sub> and three isoenzymes (S25DH<sub>2</sub>, S25DH<sub>3</sub>, and S25DH<sub>4</sub>) were overproduced in a soluble, active form allowing a straightforward purification of nontagged  $\alpha\beta\gamma$  complexes. All S25DHs contained molybdenum, four [4Fe-4S] clusters, one [3Fe-4S] cluster, and heme B and catalyzed the specific, water-dependent C-25 hydroxylations of various 4-en-3-one forms of phytosterols and zoosterols. Crude extracts from *T. aromatica* expressing genes encoding S25DH<sub>1</sub> catalyzed the hydroxylation of vitamin D<sub>3</sub> (VD<sub>3</sub>) to the clinically relevant 25-OH-VD<sub>3</sub> with >95% yield at a rate 6.5-fold higher than that of wild-type bacterial extracts; the specific activity of recombinant S25DH<sub>1</sub> was twofold higher than that of wild-type enzyme. These results demonstrate the potential application of the established expression platform for 25-OH-VD<sub>3</sub> synthesis and pave the way for the characterization of previously genetically inaccessible S25DH-like Mo enzymes of the DMSO reductase family.

**IMPORTANCE** Steroids are ubiquitous bioactive compounds, some of which are considered an emerging class of micropollutants. Their degradation by microorganisms is the major process of steroid elimination from the environment. While oxygenase-dependent steroid degradation in aerobes has been studied for more than 40 years, initial insights into the anoxic steroid degradation have only recently been obtained. Molybdenum-dependent steroid C-25 dehydrogenases (S25DHs) have been proposed to catalyze oxygen-independent side chain hydroxylations of globally abundant zoo-, phyto-, and mycosterols; however, so far, their lability has allowed only the initial characterization of a single S25DH. Here we report on a heterologous gene expression platform that allowed for easy isolation and characterization of four highly active S25DH isoenzymes. The results obtained demonstrate the key role of S25DHs during anoxic degradation of various steroids. Moreover, the platform is

Received 29 March 2018 Accepted 10 May 2018 Published 19 June 2018

**Citation** Jacoby C, Eipper J, Warnke M, Tiedt O, Mergelsberg M, Stärk H-J, Daus B, Martín-Moldes Z, Zamarro MT, Díaz E, Boll M. 2018. Four molybdenum-dependent steroid C-25 hydroxylases: heterologous overproduction, role in steroid degradation, and application for 25-hydroxyvitamin D<sub>3</sub> synthesis. mBio 9:e00694-18. <https://doi.org/10.1128/mBio.00694-18>.

**Editor** Markus W. Ribbe, University of California, Irvine

**Copyright** © 2018 Jacoby et al. This is an open-access article distributed under the terms of the [Creative Commons Attribution 4.0 International license](https://creativecommons.org/licenses/by/4.0/).

Address correspondence to Matthias Boll, [matthias.boll@biologie.uni-freiburg.de](mailto:matthias.boll@biologie.uni-freiburg.de).

valuable for the efficient enzymatic hydroxylation of vitamin D<sub>3</sub> to its clinically relevant C-25-OH form.

**KEYWORDS** alkyl hydroxylases, anaerobic catabolic pathways, molybdenum enzymes, sterols, vitamin D3 biosynthesis

**S**teroids are a ubiquitously occurring class of highly hydrophobic compounds that in eukaryotes act as hormones and essential components of biological membranes (1, 2). Due to their wide abundance and biological activity, the elimination of steroids from the environment is of global relevance (3, 4). Biodegradation of steroids is hampered by their low water solubility and by the complex tetracyclic core structure comprising quaternary carbon atoms. Only microorganisms are capable of fully degrading steroids to CO<sub>2</sub>. In the presence of oxygen, degradation of steroids heavily depends on oxygenase-dependent hydroxylation and ring cleavage reactions (5, 6).

Anaerobic steroid degradation has been studied in only a few denitrifying proteobacteria with the cholesterol-degrading *Sterolibacterium denitrificans* serving as a model organism (7). Recent studies revealed a patchwork pathway for anaerobic steroid degradation (8, 9). As in aerobic cholesterol-degrading organisms, cholest-4-en-3-one is formed as the first intermediate from cholesterol in *S. denitrificans* (Fig. 1A) (10). The subsequent hydroxylation of the side chain with water that occurs at tertiary C-25 is then catalyzed by molybdenum (Mo)-dependent steroid C-25 dehydrogenase (S25DH) (10, 11), and not at primary C-26 as observed in the oxygenase-dependent pathway. The next step involves a formal shift of the hydroxyl group from the tertiary C-25 to primary C-26 by an unknown enzyme (8, 12). Further degradation to androsta-1,4-diene-3,17-dione (ADD) proceeds via oxidation and activation to a C-26-oyl-coenzyme

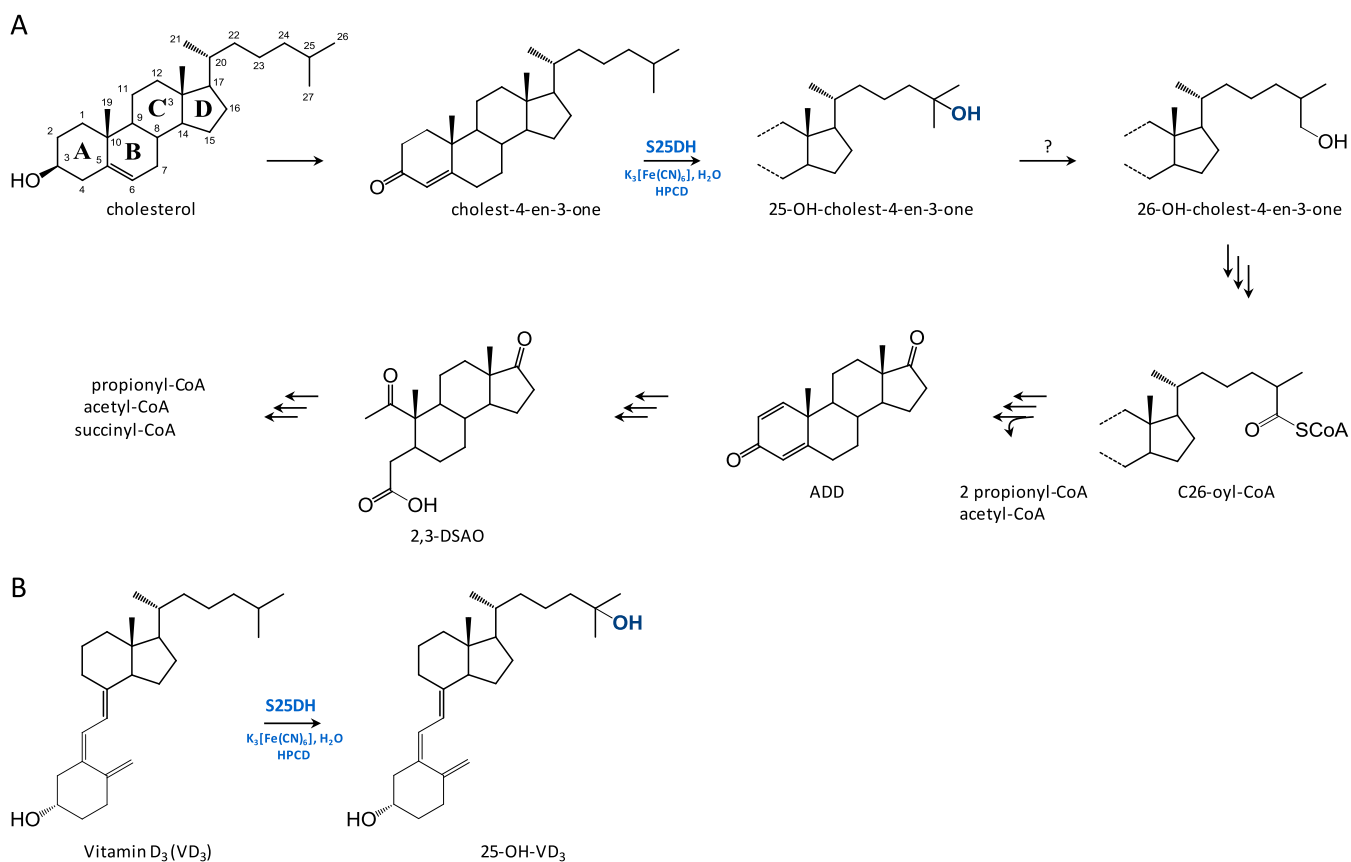


**FIG 1** (A) Proposed anoxic degradation pathway of cholesterol in *Sterolibacterium denitrificans*. The activation of the side chain is mediated by S25DH, which hydroxylates the tertiary C-25 carbon with water. ADD, androsta-1,4-diene-3-one; 2,3-DSAO, 1,17-dioxo-2,3-seco-androstan-3-oi acid. (B) Conversion of vitamin D<sub>3</sub> (VD<sub>3</sub>) to 25-OH-VD<sub>3</sub> by S25DH using ferricyanide as the electron acceptor.

A (CoA) component, followed by modified  $\beta$ -oxidation like reaction sequences (Fig. 1) (8, 13). Finally, cleavage of the sterane rings A and B proceeds in the so-called 2,3-*seco*-pathway involving ring-cleaving hydrolases (14, 15); degradation of rings C and D appears to be similar in aerobic and anaerobic steroid-degrading bacteria, again using hydrolytic enzymes (Fig. 1) (16).

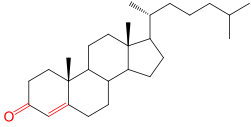
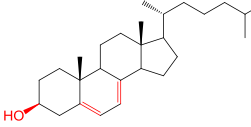
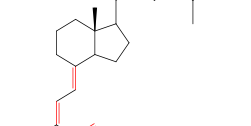
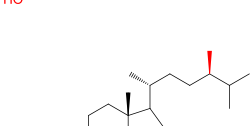
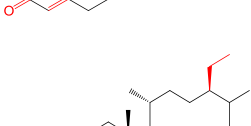
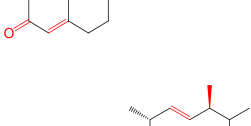
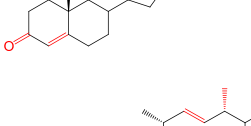
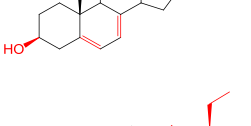
A S25DH was initially isolated and characterized by Dermer and Fuchs (11) as a molybdenum cofactor (MoCo)-containing enzyme of the dimethyl sulfoxide reductase (DMSOR) family of Mo enzymes. The enzyme has an  $\alpha\beta\gamma$  architecture comprising a 108-kDa ( $\alpha$ ), 38-kDa ( $\beta$ ), and 23-kDa ( $\gamma$ ) subunit. The catalytically active  $\alpha$ -subunit contains a molybdo-*bis*-pyranopterin guanine dinucleotide (Mo-*bis*PGD) cofactor and a [4Fe-4S] cluster; the  $\beta$ -subunit harbors four additional FeS clusters, and the  $\gamma$ -subunit contains a b-type heme. Like other members of the DMSOR family, S25DH is proposed to be located in the periplasm. It was proposed that a chaperone (SdhD) is involved in proper folding and probably in MoCo insertion (11). S25DH together with ethylbenzene dehydrogenase (EbdH) (17, 18) and *p*-cymene dehydrogenase (19) forms a phylogenetic subcluster within class II of the DMSOR family, that hydroxylate alkyl side chains of steroids or aromatic compounds with water (see Fig. S1 in the supplemental material) (20). Attempts for heterologous/homologous production of S25DH/EbdH subclass members have failed so far (21), which prevented an easy enrichment procedure, as well as the generation of molecular variants.

A recent study revealed that S25DH is capable of hydroxylating vitamin D<sub>3</sub> (VD<sub>3</sub>) to the clinically relevant 25-OH-VD<sub>3</sub> (Fig. 1B) (22). This activity was dependent on 2-hydroxypropyl- $\beta$ -cyclodextrin that is known to promote the isomerization to pre-VD<sub>3</sub> (23), the assumed actual substrate of S25DH. In contrast to cytochrome P450-dependent hydroxylation of VD<sub>3</sub>, S25DH-dependent catalysis is independent of an electron donor system and requires only the electrochemically regenerative K<sub>3</sub>[Fe(CN)<sub>6</sub>] (ferricyanide) as an electron acceptor (22). Though S25DH serves as a promising catalyst for the synthesis of 25-OH-VD<sub>3</sub>, there is a high demand for heterologous expression and for improving the enrichment of S25DH-like enzymes with regard to activities and stabilities.

*Sterolibacterium denitrificans* is capable of degrading phyto- and mycosterols such as  $\beta$ -sitosterol, stigmasterol, or ergosterol with modifications in the isoprenoid side chain (for structures, see Table 1), but the only cholest-4-en-3-one-converting S25DH studied so far is unable to convert any of the 4-en-3-one analogues of these growth substrates (8, 11). In addition to the gene encoding the active site  $\alpha$ -subunit of this S25DH (henceforth referred to as  $\alpha_1$  subunit of S25DH<sub>1</sub>, gene accession number SDENCHOL\_20805), the genome contains seven paralogous genes encoding putative S25DH-like enzymes, all affiliating with the class II DMSOR family ( $\alpha_2$ - $\alpha_8$ ) (8, 11). In particular, the predicted active site  $\alpha_{2-4}$  (amino sequence identities to  $\alpha_1$  of 72 to 82%) have been hypothesized to represent the active site subunits of S25DH<sub>2</sub>, S25DH<sub>3</sub>, and S25DH<sub>4</sub> involved in C-25 hydroxylation of steroids with modified isoprenoid side chains (Fig. 2A). This assumption is based on their differential abundance during growth on different steroids such as  $\beta$ -sitosterol or ergosterol (8); the role of the other four putative S25DHs (S25DH<sub>5</sub>, S25DH<sub>6</sub>, S25DH<sub>7</sub>, and S25DH<sub>8</sub>) is unclear (8). Notably, there are fewer genes encoding the  $\beta\gamma$ -subunit components than for the  $\alpha$ -subunits in the genome of *S. denitrificans* (Fig. 2A), suggesting that S25DHs with different  $\alpha$ -subunits share common  $\beta\gamma$ -subunit components. S25DH<sub>1</sub> from *S. denitrificans* is composed of the  $\alpha_1\beta_3\gamma_3$ -subunits (Fig. 2A). Enriched S25DH<sub>1</sub> always contained impurities of other  $\alpha$ -subunits, which made a clear assignment of activities to individual  $\alpha$ -subunits problematic (11, 22).

In this work, we aimed to elucidate the unknown function of Mo-containing S25DH isoenzymes in *S. denitrificans* in anaerobic steroid degradation and to explore their potential use for 25-OH-VD<sub>3</sub> synthesis. For this purpose, an expression platform for S25DH and related enzymes was established in the denitrifying betaproteobacterium *Thauera aromatica* yielding S25DHs with high yields and specific activities. With this

**TABLE 1** Relative activities of S25DH<sub>1</sub> in cell extracts of *Sterolibacterium denitrificans* cells grown with cholesterol compared to those in cell extracts from *T. aromatica* producing S25DH<sub>1</sub>, S25DH<sub>2</sub>, S25DH<sub>3</sub>, and S25DH<sub>4</sub>

Substrate	Chemical structure <sup>a</sup>	Relative activity of S25DH <sup>b</sup>				
		<i>S. denitrificans</i> S25DH <sub>1</sub>	<i>T. aromatica</i>			
			S25DH <sub>1</sub>	S25DH <sub>2</sub>	S25DH <sub>3</sub>	S25DH <sub>4</sub>
Cholest-4-en-3-one		100%	<b>642%</b>	<b>497%</b>	<1%	<b>288%</b>
7-dehydrocholesterol		12.7%	81.5%	<b>563%</b>	<1%	<1%
Vitamin D <sub>3</sub> (cholecalciferol)		23.7%	<b>154%</b>	32.4%	<1%	<1%
Campest-4-en-3-one		<1%	<1%	<1%	12.3%	<b>229%</b>
β-sitost-4-en-3-one		<1%	<1%	<1%	<1%	<b>191%</b>
Brassica-4-en-3-one		<1%	<1%	<1%	<1%	<1%
Ergosterol		<1%	<1%	<1%	<1%	<1%
Stigmast-4-en-3-one		<1%	<1%	<1%	<1%	<1%

<sup>a</sup>Structural differences are shown in red.<sup>b</sup>One hundred percent activity corresponds to 1.87 nmol min<sup>-1</sup> mg<sup>-1</sup> as observed for cholest-4-en-3-one conversion by extracts from wild-type bacteria grown with cholesterol. The boldface values indicate activities higher than 100%.

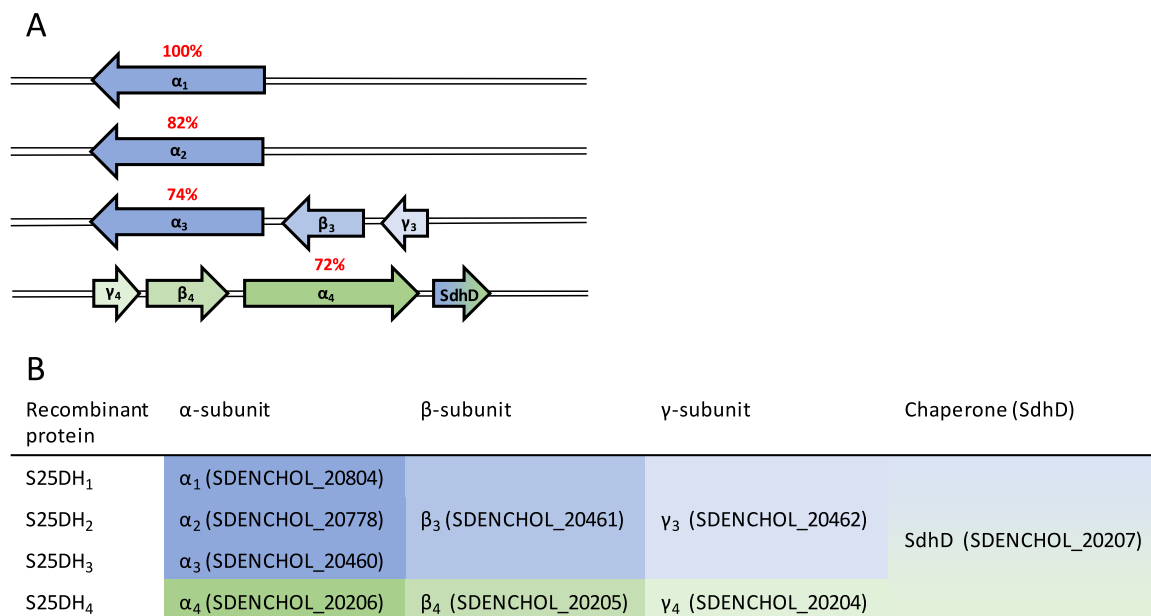


**FIG 2** Genes encoding S25DH subunits and chaperone. (A) Arrangement of genes encoding putative  $\alpha_{1-4}$  (MoCo-containing),  $\beta_{3/4}$  (4Fe-4S cluster-containing), and  $\gamma_{3,4}$  (heme b-containing) subunits, as well as the chaperone (SdhD) of S25DHs. (B) Constructs prepared for the heterologous production of S25DH<sub>1</sub>, S25DH<sub>2</sub>, S25DH<sub>3</sub>, and S25DH<sub>4</sub>.

tool, four recombinant S25DHs were isolated and characterized; their applicability as catalysts for 25-OH-VD<sub>3</sub> synthesis was probed.

## RESULTS

**Heterologous production of S25DH<sub>1</sub>.** The previously established five-step enrichment of the oxygen-sensitive S25DH<sub>1</sub> ( $\alpha_1\beta_3\gamma_3$  complex) from wild-type *Sterolibacterium denitrificans* grown with cholesterol always gave low yields, low specific activities, and a partially degraded  $\alpha_1$ -subunit (11, 22, 24). Moreover, the enriched enzyme frequently contained impurities from other S25DH  $\alpha$ -subunits next to the  $\alpha_1$ -subunit, which did not allow unambiguous assignment of activities to individual gene products (11, 22). These findings motivated us to establish a platform for actively expressing the genes encoding S25DH<sub>1</sub> and related enzymes. For this reason, the genes encoding the  $\alpha_1\beta_3\gamma_3$ -subunits, together with the putative chaperone (henceforth referred to as SdhD) (Fig. 2) were cloned into the broad-host-range plasmid pIZ1016. This construct contained the twin-arginine translocation (TAT) secretion sequence at the N terminus of the  $\alpha_1$ -subunit; to avoid any possible negative effect on  $\alpha\beta\gamma$  complex formation, we avoided the use of a tagged subunit. Heterologous production of the resulting  $\alpha_1\beta_3\gamma_3$ SdhD construct was tested in *Escherichia coli* strains BL21 and Top 10, *Azoarcus* sp. strain CIB, and *Thaueria aromatica* K172.

Heterologous production of the  $\alpha_1$ -subunit alone in the presence or absence of SdhD was not monitored in this work, as preliminary experiments indicated that such constructs did not result in the formation of soluble/active proteins. Expression of the  $\alpha_1\beta_3\gamma_3$ SdhD-encoding genes did not give soluble gene products in either of the two *E. coli* strains, and consequently, virtually no formation of 25-hydroxy-cholest-4-en-3-one was observed. However, after heterologous production of  $\alpha_1\beta_3\gamma_3$ SdhD in *Azoarcus* sp. CIB (25) and *T. aromatica* (26), anaerobically prepared cell extracts from both species showed the conversion of 0.5 mM cholest-4-en-3-one (0.5 mM) to 25-hydroxy-cholest-4-en-3-one; this conversion was dependent on time, protein,  $K_3[Fe(CN)_6]$  (5 mM), and 2-hydroxypropyl- $\beta$ -cyclodextrin (HPCD) (9% wt/vol) and was observed only with constructs containing all four  $\alpha_1\beta_3\gamma_3$ SdhD components. The specific activities of recombinant S25DH<sub>1</sub> were maximally 3.3 nmol min<sup>-1</sup> mg<sup>-1</sup> in cell extracts from *Azoarcus* sp. CIB and 12 nmol min<sup>-1</sup> mg<sup>-1</sup> in cell extracts from *T. aromatica*. Remarkably, both

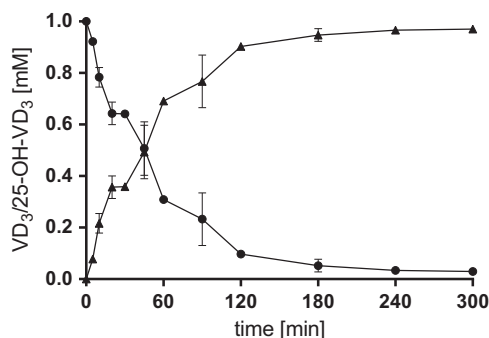


**FIG 3** Aerobic conversion of 1 mM VD<sub>3</sub> to 25-OH-VD<sub>3</sub> by crude extracts of *Thauera aromatica* K172 producing S25DH<sub>1</sub> (12 mg ml<sup>-1</sup>). Symbols: ● VD<sub>3</sub>; ▲, 25-OH-VD<sub>3</sub>.

specific activities were 176% and more than 640% of the activity in cell extracts of cholesterol-grown *S. denitrificans* (1.87 nmol min<sup>-1</sup> mg<sup>-1</sup>), respectively, demonstrating overproduction of S25DH<sub>1</sub> in the *Azoarcus* and *Thauera* species (Table 1). Under anoxic conditions, loss of recombinant S25DH<sub>1</sub> activity was less than 10% for 1 week at 4°C. In the presence of 5 mM K<sub>3</sub>[Fe(CN)<sub>6</sub>], activity in *T. aromatica* crude extracts was stable in air at 30°C for 5 to 8 h but decreased to 50% after 24 h.

*T. aromatica* crude extracts producing S25DH<sub>1</sub> catalyzed the conversion of VD<sub>3</sub> to 25-OH-VD<sub>3</sub> at 2.8 nmol min<sup>-1</sup> mg<sup>-1</sup> that was 6.5-fold higher compared to wild-type extract (0.43 nmol min<sup>-1</sup> mg<sup>-1</sup>). This increased VD<sub>3</sub> conversion rate shortened the conversion of 1 mM VD<sub>3</sub> correspondingly (90% conversion in 2 h by 12 mg ml<sup>-1</sup> crude extracts) (Fig. 3), allowing 25-OH-VD<sub>3</sub> synthesis even in air without loss of activity. The absence of 25-OH-VD<sub>3</sub>-converting enzymes in *T. aromatica* made the addition of AgNO<sub>3</sub> for blocking follow-up enzymes of the cholesterol degradation pathway dispensable (22). Recombinant S25DH also converted 7-dehydrocholesterol to its 25-OH form, as had also been reported for the wild-type enzyme (11); no analogues with modifications in the isoprenoid side chain were converted (Table 1).

**Heterologous production of S25DH<sub>2</sub>, S25DH<sub>3</sub>, and S25DH<sub>4</sub> isoenzymes in *T. aromatica*.** The results obtained indicated that *T. aromatica* K172 represents the most suitable host for the heterologous production of S25DH-like enzymes. For this reason, we used this strain for the production of three additional S25DH-like proteins that contain the α<sub>2,4</sub> active site subunits, respectively. The constructs were cloned into pIZ1016 in a manner to give S25DH<sub>2</sub>, S25DH<sub>3</sub>, and S25DH<sub>4</sub> with the compositions α<sub>2</sub>β<sub>3</sub>γ<sub>3</sub>, α<sub>3</sub>β<sub>3</sub>γ<sub>3</sub>, and α<sub>4</sub>β<sub>4</sub>γ<sub>4</sub> referred to as S25DH<sub>2</sub>, S25DH<sub>3</sub> and S25DH<sub>4</sub> (Fig. 2). Notably, the β<sub>3</sub>γ<sub>3</sub> and β<sub>4</sub>γ<sub>4</sub> subunits are almost identical (99% sequence identity), and the coexpression of their genes with those encoding individual α-subunits was chosen to facilitate the cloning procedure. In all cases, SdhD was coproduced with the individual S25DH isoenzymes.

Using cell extracts from *T. aromatica* producing the individual S25DH-like gene products, we tested the conversion of cholest-4-en-3-one, 7-dehydrocholesterol, vitamin D<sub>3</sub>, campest-4-en-3-one, brassica-4-en-3-one, ergosterol, β-sitost-4-en-3-one, and stigmat-4-en-3-one as possible substrates. The time-dependent formation of products was analyzed by ultrahigh-performance liquid chromatography (UPLC) separation coupled to diode array detection; identification was by UPLC coelution with standards in addition to electrospray ionization quadrupole time of flight mass spectrometry (ESI-QTOF-MS) detection. For UPLC chromatograms of conversions, see Fig. S2 in the supplemental material; for relative specific activities, see Table 1.

Using cell extracts of *T. aromatica* producing S25DH<sub>2</sub>, the rate of 25-OH-7-dehydrocholesterol formation was slightly higher than conversion of cholest-4-en-3-one. This extract converted VD<sub>3</sub> to 25-OH-VD<sub>3</sub> at a higher rate than *S. denitrificans* extracts grown with cholesterol, albeit the activity was only around 20% of recombinant S25DH<sub>1</sub> (Table 1). Previous differential proteome analysis showed that the α<sub>3</sub>-



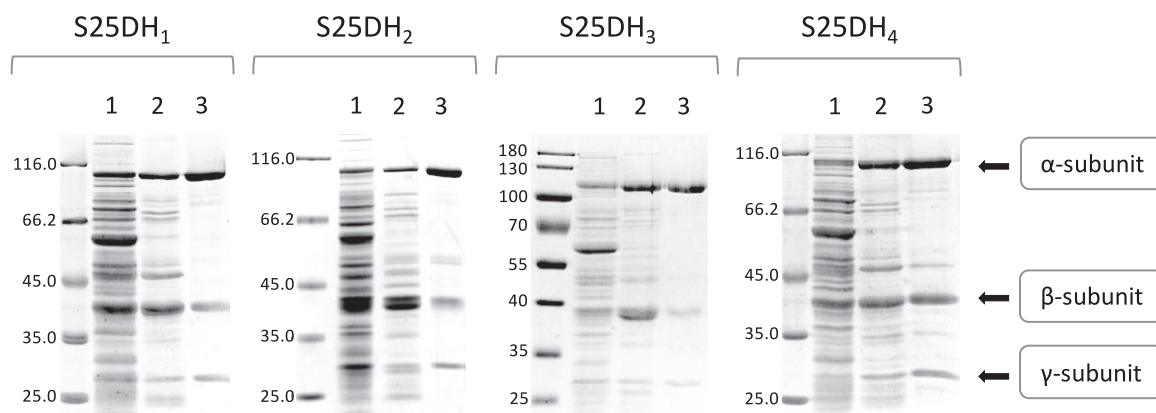


**FIG 4** Enrichment of recombinant S25DHs. SDS-PAGE analysis of S25DH activity-containing fractions during the enrichment of recombinant S25DH<sub>1</sub>, S25DH<sub>2</sub>, S25DH<sub>3</sub>, and S25DH<sub>4</sub> from *T. aromatica* cell extracts. Lane 1; 20  $\mu$ g supernatant after centrifugation at 150,000  $\times$  g; lane 2, 10  $\mu$ g protein after DEAE-Sepharose chromatography; lane 3, 5  $\mu$ g protein obtained after Reactive Red chromatography. The positions of the corresponding  $\alpha$ -,  $\beta$ - and  $\gamma$ -subunits of S25DHs are indicated by arrows to the right of the S25DH<sub>4</sub> gel. The positions of molecular size markers (in kilodaltons) are indicated to the left of the gels.

subunit of an S25DH (SDENCHOL\_20460) was most abundant during growth with ergosterol containing a  $\Delta$ 22 double bond in the side chain (8). Unexpectedly, *T. aromatica* expressing the S25DH<sub>3</sub> formed only traces of 25-OH-ergosterol from ergosterol. Likewise, brassica-4-en-3-one, an ergosterol analogue with AB rings identical to those in cholest-4-en-3-one was virtually not converted. Surprisingly, campest-4-en-3-one, which lacks the double bond in the side chain but contains an additional methyl branch at (*R*)-configured C-24, was the only steroid substrate tested that was converted by S25DH<sub>3</sub> to its 25-OH-form in significant amounts (Table 1). The  $\alpha_4$ -subunit was found upregulated in *S. denitrificans* cells grown with  $\beta$ -sitosterol, a cholesterol analogue with an additional ethyl branch at C-24 (8). In full agreement, *T. aromatica* cell extracts producing S25DH<sub>4</sub> converted  $\beta$ -sitost-4-en-3-one and the structurally related campest-4-en-3-one, both with an (*R*)-configured tertiary C-24; cholest-4-en-3-one lacking an additional alkyl substituent at this position was also converted at a slightly higher rate (Table 1).

**Enrichment, activity, and composition of recombinant S25DH<sub>2</sub>, S25DH<sub>3</sub>, and S25DH<sub>4</sub>.** The results obtained so far indicated a higher heterologous production of S25DH<sub>1</sub> and probably other S25DHs in *Azoarcus* sp. CIB and *T. aromatica* K172 than in wild-type *S. denitrificans*. As a result, only two out of five chromatographic enrichment steps described for purification from the wild-type bacteria were necessary. The two steps were DEAE anion-exchange chromatography and affinity chromatography on Reactive Red agarose (11, 22); we initially tested the purification of the recombinant S25DH<sub>1</sub> from both strains.

With *Azoarcus* sp. CIB extracts, five protein bands were obtained after the two-step purification procedure (Fig. S3). The bands migrating at 110, 40, and 25 kDa were clearly assigned to the  $\alpha_1\beta_3\gamma_3$ -subunits, whereas those migrating between 50 and 55 kDa represent truncated  $\alpha_1$  degradation products, as observed during purification from *S. denitrificans* (11, 22). The two degradation products were estimated to make more than 80% of the total amount of the  $\alpha_1$ -subunit. This finding suggests that expression in *Azoarcus* sp. CIB produced predominantly degraded S25DH<sub>1</sub> (see Fig. S3 in the supplemental material).

Purification of S25DH<sub>1</sub> from *T. aromatica* extracts revealed a highly enriched (purity >95%)  $\alpha_1\beta_3\gamma_3$  complex with an almost perfect 1:1:1 ratio of the three subunits (Fig. 4). ESI-QTOF-MS analysis of tryptic digestion products of the three excised protein bands identified the expected  $\alpha_1\beta_3\gamma_3$  subunits (see Table S1 in the supplemental material). Most importantly, when prepared from *T. aromatica* K172,  $\alpha_1$ -degradation products were negligible. These findings explain why the specific activity of recombinant S25DH<sub>1</sub>

**TABLE 2** Enrichment of four S25DHs starting from 5 g (wet weight) recombinant *T. aromatica*

Enzyme and fraction	Protein (mg)	Sp act (nmol min <sup>-1</sup> mg <sup>-1</sup> ) <sup>a</sup>	Enrichment factor	Yield (%)
<b>S25DH<sub>1</sub></b>				
Soluble fraction	645	11.2		100
DEAE + Reactive Red	6.6	395	35.3	36
<b>S25DH<sub>2</sub></b>				
Soluble fraction	546	9.3		100
DEAE + Reactive Red	9	151	16.2	27
<b>S25DH<sub>3</sub></b>				
Soluble fraction	590	0.21		100
DEAE + Reactive Red	10.2	4.6	21.9	38
<b>S25DH<sub>4</sub></b>				
Soluble fraction	552	6.4		100
DEAE + Reactive Red	10	97	15.1	27

<sup>a</sup>Specific activities were determined by the conversion of cholest-4-en-3-one for S25DH<sub>1</sub>, S25DH<sub>2</sub>, and S25DH<sub>4</sub> and of campest-4-en-3-one for S25DH<sub>3</sub>.

in *Azoarcus* sp. CIB extracts was—though still higher than in *S. denitrificans*—significantly lower than in *T. aromatica*.

Based on the results obtained with S25DH<sub>1</sub>, the S25DH<sub>2</sub>, S25DH<sub>3</sub>, and S25DH<sub>4</sub> isoenzymes were similarly purified after production of the individual enzymes in *T. aromatica*. During purification of the three S25DHs, the activity-containing fractions were assayed with the following substrates: cholest-4-en-3-one (S25DH<sub>2</sub> and S25DH<sub>4</sub>) and campest-4-en-3-one (S25DH<sub>3</sub>). In all cases, predominantly nondegraded S25DH complexes were produced; only with S25DH<sub>2</sub> a minor formation of  $\alpha_2$ -degradation products (<10%) was observed, as evidenced by a double band around 50 to 55 kDa (Fig. 4). The specific activities determined were highest with S25DH<sub>1</sub>/cholest-4-en-3-one (395 nmol min<sup>-1</sup> mg<sup>-1</sup>); the enrichment factors varied between 15-fold (S25DH<sub>4</sub>) and 38-fold (S25DH<sub>1</sub>) with yields between 27 and 38% (Table 2).

The subunit architecture and native molecular masses of the S25DHs were determined by size exclusion chromatography as follows: 167 ± 5 kDa for S25DH, S25DH<sub>2</sub>, and S25DH<sub>3</sub> and 160 ± 5 kDa for S25DH<sub>4</sub>. These values clearly point to an  $\alpha\beta\gamma$  composition of all four heterologously produced S25DHs.

**Metal content of recombinant S25DHs.** On the basis of the results of previous metal analyses with wild-type S25DH<sub>1</sub> enzyme and on the conserved binding motifs of the individual cofactors, the purified recombinant S25DH<sub>1</sub>, S25DH<sub>2</sub>, S25DH<sub>3</sub>, and S25DH<sub>4</sub> were expected to bind a Mo-*bis*PGD, four [4Fe-4S] clusters, one [3Fe-4S] cluster, and a heme b, giving one Mo atom and 20 Fe atoms per  $\alpha\beta\gamma$  trimer, respectively (11). The Fe content was analyzed by inductively coupled plasma atomic emission spectroscopy (ICP-AES), and the Mo content was analyzed by inductively coupled plasma mass spectroscopy (ICP-MS). The metal content of the four S25DHs varied between 0.5 and 0.8 Mo atoms and between 13.2 and 15.3 Fe atoms per  $\alpha\beta\gamma$  trimer, which is in the range of the values determined for the wild-type enzyme (0.7 Mo atom and 16.5 Fe atoms per enzyme) (11) (Table 3).

**Kinetic parameters of recombinant S25DH<sub>1</sub>, S25DH<sub>2</sub>, S25DH<sub>3</sub>, and S25DH<sub>4</sub>.** The  $K_m$  and  $k_{cat}$  values of each recombinant S25DH were determined using their individual preferred substrates. Notably, the  $K_m$  values determined have to be regarded as apparent values, as the nearly insoluble steroid substrates were converted only in the presence of high concentrations of the solubilizing 2-hydroxypropyl- $\beta$ -cyclodextrin (9%, wt/vol). The kinetic parameters are summarized in Table 3 with S25DH<sub>1</sub>, S25DH<sub>2</sub>, and S25DH<sub>4</sub> showing the highest  $k_{cat}/K_m$  values for cholest-4-en-3-one, 7-dehydrocholesterol, and  $\beta$ -sitost-4-en-3-one, respectively, suggesting that the respective steroids do indeed represent the preferred substrates. In the case of S25DH<sub>3</sub>, the low catalytic number



**TABLE 3** Kinetic parameters and metal content of heterologously produced S25DH<sub>1</sub>, S25DH<sub>2</sub>, S25DH<sub>3</sub>, and S25DH<sub>4</sub>

Enzyme and substrate	$K_m$ (mM) <sup>a,b</sup>	$k_{cat}$ (s <sup>-1</sup> ) <sup>a,b</sup>	$k_{cat}/K_m$ (10 <sup>3</sup> M <sup>-1</sup> s <sup>-1</sup> ) <sup>a</sup>	Mo content <sup>b,c</sup>	Fe content <sup>b,c</sup>
S25DH <sub>1</sub>					
Cholest-4-en-3-one	0.39 ± 0.08	1.11 ± 0.08	2.8	0.8 ± 0.1	15.3 ± 0.5
Vitamin D <sub>3</sub>	0.29 ± 0.09	0.23 ± 0.01	0.79		
S25DH <sub>2</sub>					
Cholest-4-en-3-one	0.124 ± 0.02	0.29 ± 0.01	2.3	0.7 ± 0.1	13.5 ± 0.8
7-Dehydrocholesterol	0.123 ± 0.02	0.33 ± 0.01	2.7		
S25DH <sub>3</sub>					
Campest-4-en-3-one	1.84 ± 0.8	0.018 ± 0.01	0.01	0.5 ± 0.1	14.2 ± 0.5
S25DH <sub>4</sub>					
Cholest-4-en-3-one	0.45 ± 0.013	0.21 ± 0.02	0.46	0.7 ± 0.1	13.2 ± 0.4
Campest-4-en-3-one	0.34 ± 0.09	0.17 ± 0.02	0.50		
β-Sitost-4-en-3-one	0.12 ± 0.01	0.14 ± 0.003	1.2		

<sup>a</sup>Kinetic parameters were determined by UPLC-based enzyme assays using different concentrations of the respective substrates in the presence of 9% (wt/vol) 2-hydroxypropyl-β-cyclodextrin.

<sup>b</sup>Mean values ± standard deviations of three biological replicates are given.

<sup>c</sup>Fe content was measured by ICP-AES, and Mo content was measured by ICP-MS. The number of Mo or Fe atoms per protein is given.

together with the high  $K_m$ , determined for campest-4-en-3-one indicates that the enzyme is specific for a so far unknown steroid, with campest-4-en-3-one representing the only analogue that is converted to some extent.

**Enrichment and characterization of S25DH<sub>4</sub> from *S. denitrificans* grown with β-sitosterol.** To ascertain whether S25DH<sub>4</sub> has an extended substrate spectrum toward β-sitost-4-en-3-one and campest-4-en-3-one, it was isolated from the wild-type bacteria. For this purpose, *S. denitrificans* was grown in a 200-liter fermenter with 3 mM β-sitosterol in a fed-batch culture, yielding 184 g cells (wet weight) (Fig. S4). Cell extracts of *S. denitrificans* grown with β-sitosterol converted β-sitost-4-en-3-one to the corresponding 25-OH-form at a specific activity of 0.6 nmol min<sup>-1</sup> mg<sup>-1</sup> (17% of the activity in recombinant *T. aromatica*).

The enrichment of β-sitost-4-en-3-one hydroxylating activity from *S. denitrificans* was based on the protocol described for S25DH<sub>1</sub> with slight modifications (see Materials and Methods). After four chromatographic steps, five dominant protein bands were found; during SDS-PAGE, these bands eluted at 110, 55, 50, 37, and 27 kDa (Fig. 5). ESI-QTOF-MS analyses of tryptic digests identified SDENCHOL\_20206 (110-, 55-, and 50-kDa bands), SDENCHOL\_20205 (37-kDa band), and SDENCHOL\_20204 (27-kDa band) (Table S2). This result indicates that the 50/55-kDa bands represent degradation subunits of the α<sub>4</sub>-subunit. Size exclusion chromatography of wild-type S25DH<sub>4</sub> revealed the same values as determined for the nontagged recombinant enzyme produced in *T. aromatica* K172, suggesting an α<sub>4</sub>β<sub>4</sub>γ<sub>4</sub> composition.

S25DH<sub>4</sub> was 55-fold enriched from *S. denitrificans* with a maximal specific activity for β-sitost-4-en-3-one conversion of 33 nmol min<sup>-1</sup> mg<sup>-1</sup>. Both wild-type and recombinant S25DH<sub>4</sub> exhibited the identical substrate preference and converted β-sitost-4-en-3-one, cholest-4-en-3-one, and campest-4-en-3-one (Table 3). In summary, the S25DH<sub>4</sub> composed of the α<sub>4</sub>β<sub>4</sub>γ<sub>4</sub> subunits has an extended substrate specificity for β-sitost-4-en-3-one (and campest-4-en-3-one); as shown for S25DH<sub>1</sub>, the specific activity of S25DH<sub>4</sub> in cell extracts was around sixfold higher when heterologously produced in *T. aromatica* compared to the wild-type S25DH<sub>4</sub>.

## DISCUSSION

So far, a number of DMSOR family members have been produced by homologously or heterologously expressing their corresponding genes (27–34). In contrast, attempts to produce the phylogenetically related, complex heterotrimeric molybdenum-iron-sulfur/heme b-containing alkyl chain hydroxylases of the class II DMSOR family in an active form have failed so far. In this work we now provide a tool for their recombinant

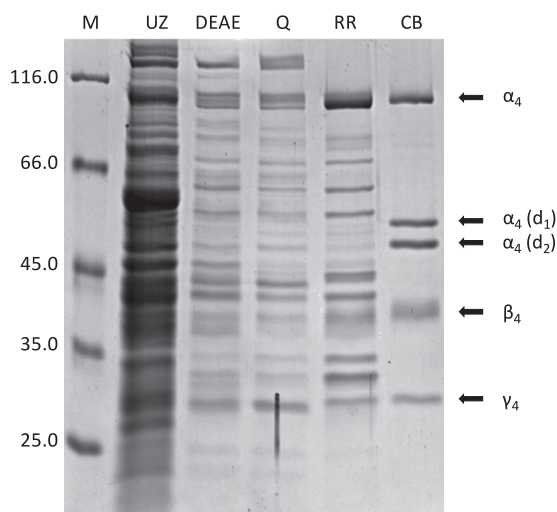


**FIG 5** Enrichment of  $\beta$ -sitost-4-en-3-one converting S25DH<sub>4</sub> from *S. denitrificans* grown with  $\beta$ -sitosterol and nitrate. Separation of protein fractions forming 25-OH- $\beta$ -sitost-4-en-3-one by 12.5% SDS-PAGE after ultracentrifugation (16  $\mu$ g of cell extract of supernatant) (UZ), chromatography on DEAE-Sepharose (24  $\mu$ g protein) (DEAE), Q-Sepharose (24  $\mu$ g protein) (Q), Reactive Red-agarose (20  $\mu$ g) (RR), and Cibacron blue-agarose (10  $\mu$ g) (CB). The arrows point to the protein bands that were identified as  $\alpha_4\beta_4\gamma_4$  of S25DH<sub>4</sub>; the proteins migrating at 50 and 55 kDa were identified as degradation products of the  $\alpha_4$ -subunit [ $\alpha_4(d_1)$  and  $\alpha_4(d_2)$ ]. Lane M contains molecular size markers (in kilodaltons).

production in highly active forms as demonstrated for the example of four S25DH isoenzymes with differing substrate specificities. The expression platform opens the door for studying other alkyl chain-hydroxylating members of the DMSOR family comprising enzymes specifically forming tertiary (S25DHs), secondary (ethylbenzene DH) (17, 18), and primary (*p*-cymene DH) (19) alcohols, and many others of unknown function. Notably, production of highly active enzymes in the presence of SdhD required the expression of all three functional genes.

Production in *Thauera aromatica* yielded crude extract activities that in the case of S25DH<sub>1</sub> and S25DH<sub>4</sub> were sixfold higher than in cell extracts from the parental *Sterolibacterium denitrificans* after growth with the preferred substrates cholesterol (S25DH<sub>1</sub>) and  $\beta$ -sitosterol (S25DH<sub>4</sub>). The apparent overexpression largely facilitated and shortened the enrichment procedure by using only two chromatographic steps, which in turn greatly reduced to a minimum the generally observed degradation of the active site  $\alpha$ -subunit. As a further advantage, the specific activities of the isolated enzymes of S25DH<sub>1</sub> and S25DH<sub>4</sub> were twofold higher than after purification from the wild type. Finally, while purification from the wild-type bacteria always yielded mixtures of different isoenzymes, the *T. aromatica* expression platform produced a preparation of a single S25DH. In summary, production in *T. aromatica* largely enhanced yield, specific activity, and specificity.

The results obtained now allow for the unambiguous assignment of substrate specificities to individual S25DH isoenzymes. The prototypical S25DH<sub>1</sub>, originally isolated from *S. denitrificans* cells grown with cholesterol (11), used cholest-4-en-3-one as the preferred substrate. The S25DH<sub>2</sub> has an extended substrate spectrum toward 7-dehydrocholesterol and S25DH<sub>4</sub> for the phytosterol-derived  $\beta$ -sitost-4-en-3-one and campest-4-en-3-one with (*R*)-configured ethyl and methyl branches at C-24, respectively. The function of S25DH<sub>3</sub> appears to be less clear, as it showed only minor activity with campest-4-en-3-one indicating that the natural substrate is still at issue. None of the four S25DHs showed significant activity with sterols containing a  $\Delta$ 22,23 double bond in the side chain such as ergosterol, brassica-4-en-3-one, or stigmast-4-en-3-one, although ergosterol and stigmasterol are growth substrates. This finding suggests that either one of the four remaining S25DHs is involved in their conversion, or a more likely alternative is that the double bond needs to be reduced or otherwise converted prior

to C-25 hydroxylation. As the abundance of S25DH<sub>3</sub> in cells grown with ergosterol was clearly increased (8), it is likely that ergosterol is first converted to a so far unknown intermediate that then serves as the substrate for S25DH<sub>3</sub>. However, reduction of the nonactivated Δ<sub>22,23</sub> double bond can hardly be achieved in the absence of oxygen with physiological electron donors. The function of S25DH<sub>5</sub>, S25DH<sub>6</sub>, S25DH<sub>7</sub>, and S25DH<sub>8</sub> needs to be elucidated in the future using the system established in this work. S25DH<sub>7</sub> has recently been proposed to be involved in the conversion of 25- to 26-OH-cholest-4-en-3-one. It is striking that the α-subunit of putative S25DH<sub>8</sub> is more closely related to that of *p*-cymene dehydrogenase and to an S25DH-like enzyme from *Thauera terpenica* (see Fig. S1 in the supplemental material), suggesting that it may play a role in hydroxylating a nonsteroidal isoprenoid compound.

This work demonstrated that of the four S25DH isoenzymes investigated in this work, S25DH<sub>1</sub> is the optimal catalyst for VD<sub>3</sub> hydroxylation to the clinically relevant 25-OH-VD<sub>3</sub> (22). This reaction is of considerable biotechnological potential, as it has several advantages in comparison to multistep chemical (35) or oxygenase- and electron donor-dependent 25-OH-VD<sub>3</sub> synthesis procedures (36–40). The established expression platform overcomes previously identified limitations of S25DH-catalyzed 25-OH-VD<sub>3</sub> synthesis, which have largely prevented biotechnological application so far. First, the easy and rapid enrichment procedure minimizes degradation of the α-subunit as always observed during purification from the wild-type strain. As a result, the specific activities of the enriched S25DHs are around twofold higher in the recombinant than in the wild-type strain. Second, S25DH<sub>1</sub> was produced to a 6.4-fold-higher extent in *T. aromatica* than in the wild-type bacteria, resulting in the corresponding increase of the VD<sub>3</sub> conversion rate in crude extracts. As a consequence, enzymatic 25-OH-VD<sub>3</sub> synthesis by crude extracts is drastically shortened and can now be accomplished even under aerobic conditions without a significant loss of activity. Third, due to the lack of enzymes catalyzing downstream reactions of anaerobic steroid degradation in *T. aromatica*, the addition of AgNO<sub>3</sub>, the established inhibitor of these reactions, is now dispensable when using crude extracts for VD<sub>3</sub> conversion.

In summary, the expression platform established in this work provides not only easy access to previously nonstudied members of the alkyl chain-hydroxylating DMSOR family members, it also allows for previously hardly achievable mechanistic studies (e.g., site-directed mutagenesis) and applied studies (25-OH-VitD<sub>3</sub> synthesis) of a catalytically versatile class of molybdenum enzymes.

## MATERIALS AND METHODS

**Chemicals and bacterial strains.** The chemicals used were of analytic grade. *Sterolibacterium denitrificans* Chol-15<sup>T</sup> (DSMZ 13999) and *Thauera aromatica* K172 (DSMZ 6984) were obtained from the Deutsche Sammlung für Mikroorganismen und Zellkulturen (DSMZ, Braunschweig, Germany). *Azoarcus* sp. strain CIB (CECT 5669) was obtained from the Spanish Type Culture Collection (Valencia, Spain), *E. coli* BL21(DE3) was from New England Biolabs (Frankfurt, Germany) and *E. coli* Top 10 was from Thermo Fisher Scientific (Carlsbad, CA).

**Synthesis of steroidal substrates.** Substrates for S25DHs were produced from commercially available steroid precursors (β-sitosterol, campesterol, brassicasterol, and stigmasterol) using cholesterol oxidase from *Streptomyces* sp. according to the manufacturer's protocol (Sisco Research Laboratories Pvt. Ltd.). The enzyme assays contained 50 mM Tris/PO<sub>4</sub> buffer (pH 7.5), 9% 2-hydroxypropyl-β-cyclodextrin (wt/vol), 2.5 mM NAD<sup>+</sup>, 1 mM substrate, 2 mM MgCl<sub>2</sub>, cholesterol oxidase, and catalase. Products were extracted and purified by high-performance liquid chromatography (HPLC) as described elsewhere (11). Samples were lyophilized and diluted in 1,4-dioxane.

**Culture conditions and preparation of cell extracts.** *S. denitrificans* was cultivated under denitrifying conditions in mineral medium with steroid substrates as described previously (7). Cells were harvested in the late exponential growth phase by centrifugation (8,000 × *g*, 20 min, 4°C). During large-scale cultivation with β-sitosterol (3 mM) in a 200-liter fermenter, nitrate was discontinuously added in 10 mM steps. *T. aromatica* K172 and *Azoarcus* sp. CIB expressing genes encoding S25DHs were cultivated under denitrifying conditions using a phosphate-buffered medium with benzoate as the carbon source at 30°C as described previously (41). Cells were harvested anaerobically by centrifugation (8,000 × *g*, 20 min, 4°C) in the late exponential phase. Frozen cells were suspended in 2 volumes of lysis buffer (wt/vol) containing 20 mM Tris/PO<sub>4</sub> (pH 7.0), 0.1 mg DNase I, 1 mM dithiothreitol (DTT), and 0.02% (wt/vol) Tween 20. Cells were lysed by passage through a French pressure cell at 137 MPa, solubilized for 3 h, and centrifuged at 150,000 × *g* for 1.5 h at 4°C. The anaerobically prepared supernatant was used for enzyme purification.

**Enzyme assays.** Enzyme assays were anaerobically carried out at 30°C in 100 mM Tris/PO<sub>4</sub> buffer (pH 7.0) with 0.5 mM steroid substrates (25 mM concentrated in 1,4-dioxane), 10 mM K<sub>3</sub>[Fe(CN)<sub>6</sub>], and 9% 2-hydroxypropyl- $\beta$ -cyclodextrin (wt/vol) following substrate consumption and product formation by ultrahigh-performance liquid chromatography (UPLC) as described previously (11, 22). For the conversion of cholest-4-en-3-one with cell extracts of *S. denitrificans*, 0.5 mM AgNO<sub>3</sub> were added to prevent further oxidation of the substrate.

**Heterologous gene expression and S25DH production.** The genes encoding the  $\alpha\beta\gamma$ -subunits together with the chaperone (SdhD) were amplified by PCR from *S. denitrificans* genomic DNA as the template, using primers suitable for T4 ligation (see Table S3 in the supplemental material). Genes encoding  $\gamma_3\beta_3$ -subunits were amplified together by using S25DH $\gamma_3\beta_3$ \_for (for stands for forward) and S25DH $\gamma_3\beta_3$ \_rev (rev stands for reverse) primers, and the resulting 1.8-kb DNA fragment was ClaI/HindIII doubly digested; the genes encoding  $\alpha_1$  and  $\alpha_3$ -subunits were amplified by using S25DH $\alpha_{1-3}$ \_for and S25DH $\alpha_{1-3}$ \_rev primers, generating a 2.9-kb DNA fragment that was HindIII/SpeI doubly digested. The gene encoding SdhD was amplified using SdhD\_for and SdhD\_rev primers, generating a 0.9-kb DNA fragment that was SpeI/XbaI doubly digested. All fragments were sequentially cloned into the broad-host-range vector pIZ1016 (Gm<sup>r</sup>, *ori*pBBR1, Mob<sup>+</sup>, *lacZ* $\alpha$ , *Pta*/*lacI*<sup>q</sup>), a derivative of pBBR1MCS-5, bearing the *tac* promoter and *lacI*<sup>q</sup> regulatory gene from pMM40 (42), and transformed in *E. coli* NEB5 $\alpha$  (New England Biolabs GmbH) according to the manufacturer's protocol. Genes encoding the  $\alpha_4\beta_4\gamma_4$ -SdhD components of S25DH<sub>4</sub> were amplified with specific primers suitable for Gibson assembly (Table S3) using the Gibson Assembly master mix (New England Biolabs GmbH) at 50°C for 1 h. The following steps are described for *T. aromatica* but were also similarly applied for *Azoarcus* sp. CIB. The genes were transformed into *T. aromatica* cells by electroporation as follows: *T. aromatica* was cultivated on phosphate-buffered medium (25 mM acetate) at 30°C until it reached an optical density at 578 nm (OD<sub>578</sub>) of 0.4 to 0.6, centrifuged (4,500  $\times$  g, 15 min, 4°C), and washed twice in 20% volume ice-cold 1 mM morpholinepropanesulfonic acid (MOPS) buffer. Centrifuged cells (4,500  $\times$  g, 15 min, 4°C) were suspended in 0.5% volume ice-cold 1 mM MOPS–15% glycerol (wt/vol). Cells were immediately used for transformation at 1.7 kV (Eppendorf Eporator) and incubated in medium at 30°C for 4 h before plated on selection medium (0.8% Gelrite, 0.025% MgSO<sub>4</sub> · 7H<sub>2</sub>O, 25 mM acetate, and 20  $\mu$ g ml<sup>-1</sup> gentamicin). Cultivation was carried out aerobically at 30°C until colonies were formed. For gene expression, cells were grown under denitrifying conditions in phosphate-buffered medium with benzoate as the carbon source (see above) supplemented with 20  $\mu$ g ml<sup>-1</sup> gentamicin. Expression of S25DH genes was fostered by adding 1 mM IPTG at an optical density of 0.7. After subsequent growth for 48 h, cells were harvested anaerobically in the late exponential phase. For gene expression of S25DH<sub>1</sub> in *E. coli* BL21 and *E. coli* Top 10, cells were cultivated anaerobically (25 mM nitrate) at 30°C in M4 minimal medium and aerobically in 2 $\times$  YT medium at 20°C complemented with 20  $\mu$ g ml<sup>-1</sup> gentamicin.

**Enrichment of recombinant proteins from *T. aromatica*.** After ultracentrifugation (150,000  $\times$  g, 1.5 h, 4°C), the soluble protein fraction was applied to a DEAE-Sepharose column under anaerobic conditions (50 ml; GE Healthcare) at 5 ml min<sup>-1</sup> and washed with buffer A (20 mM Tris/PO<sub>4</sub> [pH 7.0], 1 mM DTT, and 0.02% [wt/vol] Tween 20). The soluble protein fraction was eluted by increasing the amount of buffer B (20 mM Tris/PO<sub>4</sub> [pH 7.0], 1 mM DTT, 0.02% [wt/vol] Tween 20, and 500 mM KCl) from 12% to 16%. Active fractions were concentrated (30-kDa cutoff membrane), diluted in 10 volumes of buffer C (20 mM Tris/morpholineethanesulfonic acid [MES] [pH 6.0], 1 mM DTT), and applied to a Reactive Red 120 column (50 ml; GE Healthcare) at 5 ml min<sup>-1</sup>. The active fractions were elute with an increasing gradient of buffer D from 0 to 100% (Tris/PO<sub>4</sub> [pH 8.0], 1 mM DTT) in 20% steps. S25DH<sub>1</sub>, S25DH<sub>2</sub>, S25DH<sub>3</sub>, and S25DH<sub>4</sub> eluted at pH values of approximately 6.5, 6.7, 7.5, and 7.8, respectively.

**Purification of S25DH<sub>4</sub> from *S. denitrificans*.** Soluble proteins were applied to a DEAE Sepharose column at 1.5 ml min<sup>-1</sup> and washed with buffer A. Column-bound proteins were enriched using a stepwise gradient (10%) of buffer B from 10% to 20%. The active fraction was diluted 1:3 with buffer A and applied to a Q-Sepharose column (20 ml; GE Healthcare) at 0.5 ml min<sup>-1</sup>. The active fraction was eluted by a gradient of buffer C<sub>2</sub> (20 mM MES/Tris [pH 6.0], 1 mM DTT, 0.02% Tween 20, and 500 mM KCl) from 10% to 20%. The active fractions were diluted in 1:10 in buffer C and applied to a Reactive Red 120 column at 0.5 ml min<sup>-1</sup>. The active fractions were eluted by increasing the concentration of buffer C<sub>2</sub> from 80% to 100%. Activity-containing fractions were concentrated, desalted, and screened for activity. Active fractions were applied to a Cibacron blue-Sepharose column (1 ml; GE Healthcare) at 0.5 ml min<sup>-1</sup> using buffer C. The active fractions were eluted by increasing the concentration of buffer D in 20% steps from 80% to 100%. The active fractions were pooled and concentrated (30-kDa cutoff membrane).

**Determination of Mo and Fe content by ICP-MS/ICP-AES.** Inductively coupled plasma mass spectroscopy (ICP-MS)/inductively coupled plasma atomic emission spectroscopy (ICP-AES) analyses were conducted to determine the Mo and Fe content of heterologously produced S25DHs as described previously (43).

**Gel filtration.** The native molecular weight of steroid C-25 dehydrogenases was analyzed by size exclusion chromatography on a Superdex 200 column (GE Healthcare) at 0.5 ml min<sup>-1</sup> in 50 mM Tris-HCl (pH 7.0)–150 mM NaCl. Proteins used for calibration were thyroglobulin (669 kDa), apoferritin (443 kDa), alcohol dehydrogenase (150 kDa), carbonic anhydrase (29 kDa), and cytochrome c (12.4 kDa).

**Protein identification by mass spectrometry.** Proteins were identified by excising the bands of interest from an SDS-PAGE. After in-gel digestion with trypsin (Sigma-Aldrich), the resulting peptides were separated by UPLC and identified by using a Synapt G2-Si high-definition mass spectrometry (HDMS) electrospray ionization quadrupole time of flight (ESI-QTOF) system (Waters) as described previously (44).

## SUPPLEMENTAL MATERIAL

Supplemental material for this article may be found at <https://doi.org/10.1128/mBio.00694-18>.

**FIG S1**, PDF file, 0.5 MB.

**FIG S2**, PDF file, 0.2 MB.

**FIG S3**, PDF file, 0.2 MB.

**FIG S4**, PDF file, 0.2 MB.

**TABLE S1**, DOCX file, 0.01 MB.

**TABLE S2**, DOCX file, 0.01 MB.

**TABLE S3**, DOCX file, 0.01 MB.

## ACKNOWLEDGMENTS

This work was funded by the Germany Research Foundation DFG (BO 1565, 15-1) and by the Ministry of Economy and Competitiveness of Spain (BIO2016-79736-R).

## REFERENCES

- Dufourc EJ. 2008. Sterols and membrane dynamics. *J Chem Biol* 1:63–77. <https://doi.org/10.1007/s12154-008-0010-6>.
- Nes WD. 2011. Biosynthesis of cholesterol and other sterols. *Chem Rev* 111:6423–6451. <https://doi.org/10.1021/cr200021m>.
- Barbosa MO, Moreira NFF, Ribeiro AR, Pereira MFR, Silva AMT. 2016. Occurrence and removal of organic micropollutants: an overview of the watch list of EU Decision 2015/495. *Water Res* 94:257–279. <https://doi.org/10.1016/j.watres.2016.02.047>.
- Ting YF, Praveena SM. 2017. Sources, mechanisms, and fate of steroid estrogens in wastewater treatment plants: a mini review. *Environ Monit Assess* 189:178. <https://doi.org/10.1007/s10661-017-5890-x>.
- Bergstrand LH, Cardenas E, Holert J, Van Hamme JD, Mohn WW. 2016. Delineation of steroid-degrading microorganisms through comparative genomic analysis. *mBio* 7:e00166. <https://doi.org/10.1128/mBio.00166-16>.
- Kieslich K. 1985. Microbial side chain degradation of sterols. *J Basic Microbiol* 25:461–474. <https://doi.org/10.1002/jobm.3620250713>.
- Tarlera S, Denner EB. 2003. *Sterolibacterium denitrificans* gen. nov., sp. nov., a novel cholesterol-oxidizing, denitrifying member of the beta-Proteobacteria. *Int J Syst Evol Microbiol* 53:1085–1091. <https://doi.org/10.1099/ijs.0.02039-0>.
- Warnke M, Jacoby C, Jung T, Agne M, Mergelsberg M, Starke R, Jehmlich N, von Bergen M, Richnow HH, Brüls T, Boll M. 2017. A patchwork pathway for oxygenase-independent degradation of side chain containing sterols. *Environ Microbiol* 19:4684–4699. <https://doi.org/10.1111/1462-2920.13933>.
- Yang FC, Chen YL, Tang SL, Yu CP, Wang PH, Ismail W, Wang CH, Ding JY, Yang CY, Yang CY, Chiang YR. 2016. Integrated multi-omics analyses reveal the biochemical mechanisms and phylogenetic relevance of anaerobic androgen biodegradation in the environment. *ISME J* 10:1967–1983. <https://doi.org/10.1038/ismej.2015.255>.
- Chiang YR, Ismail W, Müller M, Fuchs G. 2007. Initial steps in the anoxic metabolism of cholesterol by the denitrifying *Sterolibacterium denitrificans*. *J Biol Chem* 282:13240–13249. <https://doi.org/10.1074/jbc.M610963200>.
- Dermer J, Fuchs G. 2012. Molybdoenzyme that catalyzes the anaerobic hydroxylation of a tertiary carbon atom in the side chain of cholesterol. *J Biol Chem* 287:36905–36916. <https://doi.org/10.1074/jbc.M112.407304>.
- Wang PH, Lee TH, Ismail W, Tsai CY, Lin CW, Tsai YW, Chiang YR. 2013. An oxygenase-independent cholesterol catabolic pathway operates under oxic conditions. *PLoS One* 8:e66675. <https://doi.org/10.1371/journal.pone.0066675>.
- Warnke M, Jung T, Jacoby C, Agne M, Feller FM, Philipp B, Seiche W, Breit B, Boll M. 2018. Functional characterization of three specific acyl-coenzyme A synthetases involved in anaerobic cholesterol degradation in *Sterolibacterium denitrificans* Chol15. *Appl Environ Microbiol* 84:e02721-17. <https://doi.org/10.1128/AEM.02721-17>.
- Wang PH, Leu YL, Ismail W, Tang SL, Tsai CY, Chen HJ, Kao AT, Chiang YR. 2013. Anaerobic and aerobic cleavage of the steroid core ring structure by *Steroidobacter denitrificans*. *J Lipid Res* 54:1493–1504. <https://doi.org/10.1194/jlr.M034223>.
- Wang PH, Yu CP, Lee TH, Lin CW, Ismail W, Wey SP, Kuo AT, Chiang YR. 2014. Anoxic androgen degradation by the denitrifying bacterium *Sterolibacterium denitrificans* via the 2,3-seco pathway. *Appl Environ Microbiol* 80:3442–3452. <https://doi.org/10.1128/AEM.03880-13>.
- Crowe AM, Casabon I, Brown KL, Liu J, Lian J, Rogalski JC, Hurst TE, Snieckus V, Foster LJ, Eltis LD. 2017. Catabolism of the last two steroid rings in *Mycobacterium tuberculosis* and other bacteria. *mBio* 8:e00321-17. <https://doi.org/10.1128/mBio.00321-17>.
- Kniemeyer O, Heider J. 2001. Ethylbenzene dehydrogenase, a novel hydrocarbon-oxidizing molybdenum/iron-sulfur/heme enzyme. *J Biol Chem* 276:21381–21386. <https://doi.org/10.1074/jbc.M101679200>.
- Johnson HA, Pelletier DA, Spormann AM. 2001. Isolation and characterization of anaerobic ethylbenzene dehydrogenase, a novel Mo-Fe-S enzyme. *J Bacteriol* 183:4536–4542. <https://doi.org/10.1128/JB.183.15.4536-4542.2001>.
- Strijkstra A, Trautwein K, Jarling R, Wöhlbrand L, Dörries M, Reinhardt R, Drozdowska M, Golding BT, Wilkes H, Rabus R. 2014. Anaerobic activation of p-cymene in denitrifying betaproteobacteria: methyl group hydroxylation versus addition to fumarate. *Appl Environ Microbiol* 80:7592–7603. <https://doi.org/10.1128/AEM.02385-14>.
- Grimaldi S, Schoepp-Cothenet B, Ceccaldi P, Guigliarelli B, Magalon A. 2013. The prokaryotic Mo/W-bisPGD enzymes family: a catalytic workhorse in bioenergetic. *Biochim Biophys Acta* 1827:1048–1085. <https://doi.org/10.1016/j.bbabi.2013.01.011>.
- Rugor A, Wójcik-Augustyn A, Niedzialkowska E, Mordalski S, Staroń J, Bogarski A, Szaleniec M. 2017. Reaction mechanism of sterol hydroxylation by steroid C25 dehydrogenase—homology model, reactivity and isoenzymatic diversity. *J Inorg Biochem* 173:28–43. <https://doi.org/10.1016/j.jinorgbio.2017.04.027>.
- Warnke M, Jung T, Dermer J, Hipp K, Jehmlich N, von Bergen M, Ferlino S, Fries A, Müller M, Boll M. 2016. 25-Hydroxyvitamin D3 synthesis by enzymatic steroid side-chain hydroxylation with water. *Angew Chem Int Ed Engl* 55:1881–1884. <https://doi.org/10.1002/anie.201510331>.
- Tian XQ, Holick MF. 1995. Catalyzed thermal isomerization between previtamin D<sub>3</sub> and vitamin D<sub>3</sub> via beta-cyclodextrin complexation. *J Biol Chem* 270:8706–8711. <https://doi.org/10.1074/jbc.270.15.8706>.
- Rugor A, Tataruch M, Staroń J, Dudzik A, Niedzialkowska E, Nowak P, Högendorf A, Michalik-Zym A, Napruszewska DB, Jarzębski A, Szymańska K, Białas W, Szaleniec M. 2017. Regioselective hydroxylation of cholecalciferol, cholesterol and other sterol derivatives by steroid C25 dehydrogenase. *Appl Microbiol Biotechnol* 101:1163–1174. <https://doi.org/10.1007/s00253-016-7880-2>.
- Martin-Moldes Z, Zamarro MT, Del Cerro C, Valencia A, Gómez MJ, Arcas A, Udaondo Z, García JL, Nogales J, Carmona M, Díaz E. 2015. Whole-genome analysis of *Azoarcus* sp. strain CIB provides genetic insights to its different lifestyles and predicts novel metabolic features. *Syst Appl Microbiol* 38:462–471. <https://doi.org/10.1016/j.syapm.2015.07.002>.
- Anders HJ, Kaetzke A, Kampfer P, Ludwig W, Fuchs G. 1995. Taxonomic position of aromatic-degrading denitrifying pseudomonad strains K 172 and KB 740 and their description as new members of the genera *Thaueria*, as *Thaueria aromatica* sp. nov., and *Azoarcus*, as *Azoarcus evansii* sp. nov., respectively, members of the beta subclass of the *Proteobacteria*. *Int J Syst Bacteriol* 45:327–333. <https://doi.org/10.1099/00207713-45-2-327>.



27. Chu S, Zhang D, Wang D, Zhi Y, Zhou P. 2017. Heterologous expression and biochemical characterization of assimilatory nitrate and nitrite reductase reveals adaptation and potential of *Bacillus megaterium* NCT-2 in secondary salinization soil. *Int J Biol Macromol* 101:1019–1028. <https://doi.org/10.1016/j.ijbiomac.2017.04.009>.
28. Hartmann T, Leimkühler S. 2013. The oxygen-tolerant and NAD<sup>+</sup>-dependent formate dehydrogenase from *Rhodobacter capsulatus* is able to catalyze the reduction of CO<sub>2</sub> to formate. *FEBS J* 280:6083–6096. <https://doi.org/10.1111/febs.12528>.
29. Hilton JC, Temple CA, Rajagopalan KV. 1999. Re-design of *Rhodobacter sphaeroides* dimethyl sulfoxide reductase. Enhancement of adenosine N1-oxide reductase activity. *J Biol Chem* 274:8428–8436. <https://doi.org/10.1074/jbc.274.13.8428>.
30. Kappler U, McEwan AG. 2002. A system for the heterologous expression of complex redox proteins in *Rhodobacter capsulatus*: characterisation of recombinant sulphite:cytochrome c oxidoreductase from *Starkeya novella*. *FEBS Lett* 529:208–214. [https://doi.org/10.1016/S0014-5793\(02\)03344-6](https://doi.org/10.1016/S0014-5793(02)03344-6).
31. Malasarn D, Keeffe JR, Newman DK. 2008. Characterization of the arsenate respiratory reductase from *Shewanella* sp. strain ANA-3. *J Bacteriol* 190:135–142. <https://doi.org/10.1128/JB.01110-07>.
32. Pollock VV, Conover RC, Johnson MK, Barber MJ. 2002. Bacterial expression of the molybdenum domain of assimilatory nitrate reductase: production of both the functional molybdenum-containing domain and the nonfunctional tungsten analog. *Arch Biochem Biophys* 403:237–248. [https://doi.org/10.1016/S0003-9861\(02\)00215-1](https://doi.org/10.1016/S0003-9861(02)00215-1).
33. Tenbrink F, Schink B, Kroneck PM. 2011. Exploring the active site of the tungsten, iron-sulfur enzyme acetylene hydratase. *J Bacteriol* 193:1229–1236. <https://doi.org/10.1128/JB.01057-10>.
34. Wu SY, Rothery RA, Weiner JH. 2015. Pyranopterin coordination controls molybdenum electrochemistry in *Escherichia coli* nitrate reductase. *J Biol Chem* 290:25164–25173. <https://doi.org/10.1074/jbc.M115.665422>.
35. Zhu GD, Okamura WH. 1995. Synthesis of vitamin D (calciferol). *Chem Rev* 95:1877–1952. <https://doi.org/10.1021/cr00038a007>.
36. Hayashi K, Yasuda K, Sugimoto H, Ikushiro S, Kamakura M, Kittaka A, Horst RL, Chen TC, Ohta M, Shiro Y, Sakaki T. 2010. Three-step hydroxylation of vitamin D<sub>3</sub> by a genetically engineered CYP105A1: enzymes and catalysis. *FEBS J* 277:3999–4009. <https://doi.org/10.1111/j.1742-4658.2010.07791.x>.
37. Kang DJ, Im JH, Kang JH, Kim KH. 2015. Bioconversion of vitamin D<sub>3</sub> to calcifediol by using resting cells of *Pseudonocardia* sp. *Biotechnol Lett* 37:1895–1904. <https://doi.org/10.1007/s10529-015-1862-9>.
38. Sakaki T, Sugimoto H, Hayashi K, Yasuda K, Munetsuna E, Kamakura M, Ikushiro S, Shiro Y. 2011. Bioconversion of vitamin D to its active form by bacterial or mammalian cytochrome P450. *Biochim Biophys Acta* 1814:249–256. <https://doi.org/10.1016/j.bbapap.2010.07.014>.
39. Yasuda K, Endo M, Ikushiro S, Kamakura M, Ohta M, Sakaki T. 2013. UV-dependent production of 25-hydroxyvitamin D<sub>2</sub> in the recombinant yeast cells expressing human CYP2R1. *Biochem Biophys Res Commun* 434:311–315. <https://doi.org/10.1016/j.bbrc.2013.02.124>.
40. Yasutake Y, Nishioka T, Imoto N, Tamura T. 2013. A single mutation at the ferredoxin binding site of P450 Vdh enables efficient biocatalytic production of 25-hydroxyvitamin D<sub>3</sub>. *Chembiochem* 14:2284–2291. <https://doi.org/10.1002/cbic.201300386>.
41. Tschuch A, Fuchs G. 1987. Anaerobic degradation of phenol by pure cultures of newly isolated denitrifying pseudomonads. *Arch Microbiol* 148:213–217. <https://doi.org/10.1007/BF00414814>.
42. Kovach ME, Elzer PH, Hill DS, Robertson GT, Farris MA, Roop RM, Peterson KM. 1995. Four new derivatives of the broad-host-range cloning vector pBBR1MCS, carrying different antibiotic-resistance cassettes. *Gene* 166:175–176. [https://doi.org/10.1016/0378-1119\(95\)00584-1](https://doi.org/10.1016/0378-1119(95)00584-1).
43. Weinert T, Huwiler SG, Kung JW, Weidenweber S, Hellwig P, Stärk HJ, Biskup T, Weber S, Cotelesage JJ, George GN, Ermiler U, Boll M. 2015. Structural basis of enzymatic benzene ring reduction. *Nat Chem Biol* 11:586–591. <https://doi.org/10.1038/nchembio.1849>.
44. Mergelsberg M, Willistein M, Meyer H, Stärk HJ, Bechtel DF, Pierik AJ, Boll M. 2017. Phthaloyl-CoA decarboxylase from *Thaueria chlorobenzoica*: the prenylated flavin, K<sup>+</sup>, and Fe<sup>2+</sup>-dependent key enzyme of anaerobic phthalate degradation. *Environ Microbiol* 19:3734–3744. <https://doi.org/10.1111/1462-2920.13875>.